10.21611/qirt.2016.062

Thermographic detection of abraded pipeline walls in the industrial installations

by M. Kopeć, B. Więcek

Lodz Univ. of Technology, 90-924, Wolczanska Str., Lodz, Poland, *michal.kopec@dokt.p.lodz.pl, boguslaw.wiecek@p.lodz.pl*

Abstract

The aim of this paper is to develop a new method for detection of abraded walls in the industrial pipelines. The reason of the reduction of pipelines wall thickness is mainly long time exploitation. Also high temperature and variable pressure of the transported medium cause of faster walls abrasion process in the pipelines. Too long exploitation can lead to break a pipeline's wall, and in the case of a dangerous gas it may lead to an explosion. The presented results show the dependence between surface temperature and a wall thickness of the pipeline.

1. Introduction

Ensuring continuous operation is a priority for all companies. For many years, the industrial pipelines have become the low-cost and low-price method for transport various types of the substances. In last three decades the number of transmission pipelines rapidly increased [1]. Therefore the failures can occur more frequently. In industry, even a short break in the production and continuous operations can cause the financial losses. For this reason the replacement or renewal of the pipeline should be made after detailed assessment of their technical condition and risk of economic analysis for further exploitation. The article focuses on the assessment of possibility break of a wall in the pipelines, especially on the bend segment. The knowledge of the pipeline wall thickness is the very important factor, particularly in transmission pipelines of dangerous gases or liquids networks. The pipelines are repeatedly under influence of negative interactions of the transported medium [2]. The reason of thinning of pipeline's wall is mainly the long exploitation time. The structural components of the pipelines are destroyed as a result of continuous exploitation, which influences on the durability of the element. Also high temperature and varying pressure of the transported medium is one of the cause of faster walls abrasion process in the pipelines. A microstructure of the pipeline wall is degraded by long operation time and the material pits are formed, as a result of the internal pressure changes and district stresses [3,4].

There are many factors having the influence on the efficiency and life-time of the pipeline, such as: creep, friction, corrosion, gouge, mechanical and thermal fatigue. The creep is a fundamental process, which determine the mechanical behavior of the material at higher temperature. In some cases it may occurs endothermic reaction which leads to a negative balance of the heat transfer, i.e. heat absorption from the environment. Therefore, the materials used for the construction of the pipelines should have the required material deformation strength at higher temperature and should not be susceptible to break. Unexpected damage to a pipe may have significant impact on society and environment. It requires the appropriate management and systematic maintenance of the pipelines. Thus, the management of the pipeline requires regular inspections and every kind of the degradation, which could worsen the system reliability, its components and structures should be closely monitored in order to take timely actions.

The aim of this paper is to work out a reliable method for determining quantitatively of the material actual condition in order to predict the durability of the pipelines in the exploitation conditions. The authors analyzed surface temperature of the tested material in quasi-static condition, for the example of the pipeline's knees transporting the hot gas (in this research air). In this work, the thermovision was applied to the measure the time-dependent thermal process. The thermovision is a radiation testing method. It uses the appropriate and advanced methodology and software for the analysis. At this point one should notice, that the thermovision is the non-destructive methods. The non-destructive method is relatively safe and enables the measurement in a quick and easy manner [5].

The results of this study have the practical aspect. Now, there is a demand for such methods, which can be used for the inspection permanent in industry. The presented results of the analysis indicate the possibility of determining quantitatively the pipeline wall thickness. The thinned-wall of the pipeline induces temperature differences on the surface of the tested object. Until now, it wasn't elaborated generally accepted standards and instructions for the assessment of the pipe degradation degree in the industrial installations. Therefore, such methods are not generally accepted and they need a severe testing and approval. Currently applied diagnostic methods use different criteria for the assessment of the material. Typically, these methods are comparable but they give often significantly different results [6]. The review of the literature confirmed absence the thermovision methods to determine of the pipeline wall thickness and this is the originality of the article. The quantitative determination of wall thickness is difficult, because changes in the material structure not depends on temperature only, but on other factors.

10.21611/qirt.2016.062

2. Materials and methods

The authors elaborated the test rig shown in fig. 1 where the tested objects are the PolyPropylene knees (PP) of different wall thickness. The producer ensures that his products are compatible with EN1451 norm concerning the strength, temperature and life-time. The material is suited to the operation up to 90°C. The tested objects are characterized by smooth outside wall. In this case the PP knee reflects bend of the pipeline. These knees have 75 mm diameter and 87,5° deflection angle. As a medium source, a controlled hot air stream was chosen.

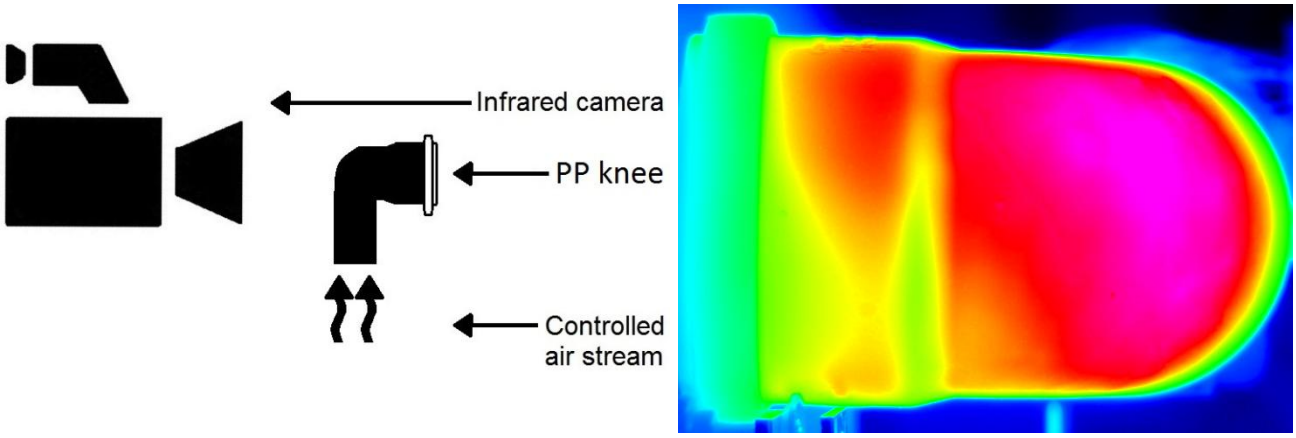

(a) (b)

Fig. 1. *The measurement test rig (a) and an exemplary thermal image (b) chosen from the sequence recorded for the heating process*

The thermal responses of the tested material were measured using *Cedip Titanium* infrared thermographic camera, with the cooled *InSb* FPA detector of the size 640 x 512 pixels with *NETD* = 20mK. The thermograms acquisition was made using the camera dedicated control program (*Altair* software [7]), that runs on a PC. The exemplary thermogram is shown in fig. 1b. One observed the pipeline area with the largest possible defect. This place is was on the bend of the pipeline. In fig. 2,5 and 6, we presented thermal characteristics of the analyzed data. The different curves correspond to pipes with different wall thickness. The dynamic and static behavior is represented by the curves in fig. 2, where the change of the temperature is plotted as a function of time. It is the response at the step-function power excitation. The heating curves have been transformed into the Nyquist plots (fig. 6). The Nyquist diagram is the thermal impedance of the object as function of frequency using the Fourier transform. – real and the imaginary parts of the impedance [11]. The time constant can be easily determined using deconvolution. (fig. 5).

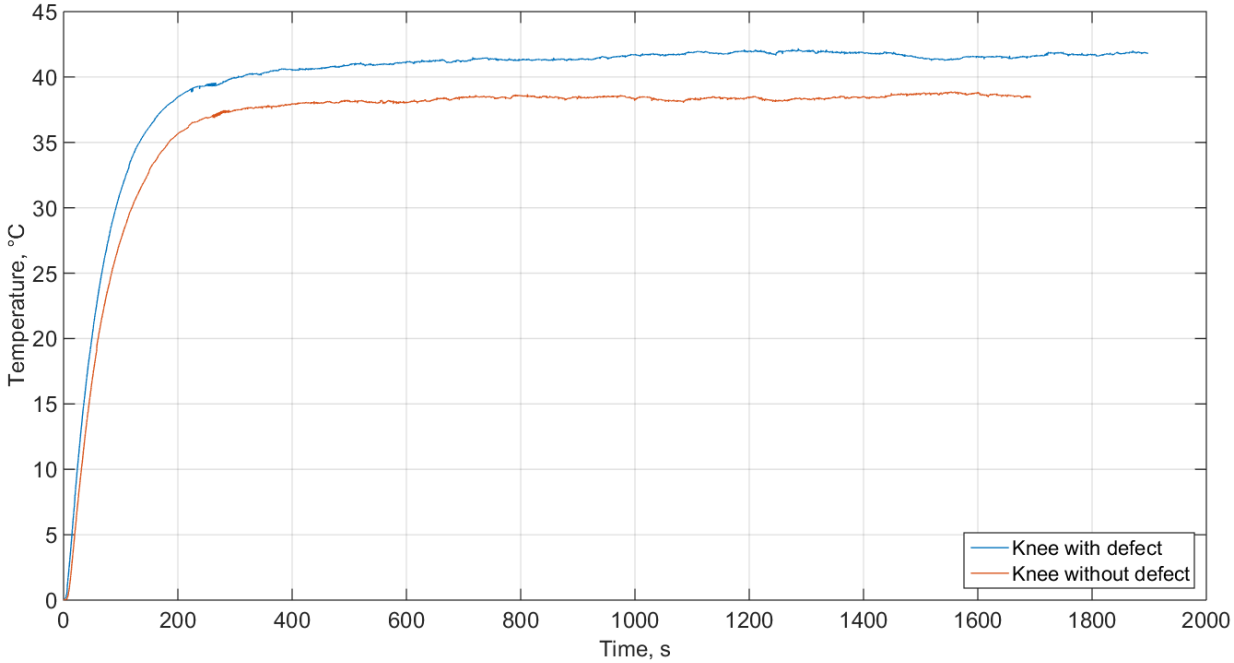

Fig. 2. *The heating curves for the both tested objects*

In order to investigate the dynamic behavior of the tested objects, the thermal transient temperature characteristics have been measured. The data were analyzed with using T3Ster thermal transient tester equipment [8,9] and Matlab software [10]. The way for the characterization of the transient thermal behavior of an electronic device is using a thermal transient tester equipment [11]. The dynamic thermal behavior can be described in two ways: in time and in the frequency domains. In the time domain, the thermal step response is used. The heating curves are used in time domain while in frequency domain the complex impedances are analyzed.

One can notice that the thermal system should be described with arbitrarily chosen fine resolution. In our approach, heat flows mainly in one direction [12]. The dynamic behavior of the lumped parameter RC circuits can be characterized by a set of τ_N time-constants and the related R_{thN} magnitudes. These data can be easily turned into a model network [9].

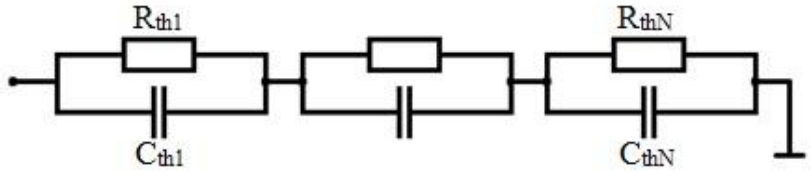

Fig. 3. *Foster model of physical structure with finite time constants [9]*

This network is shown in fig. 3, where the resistances are equal to the magnitudes of the time constants intensity and together with the thermal capacities, one can determine the thermal time constants.

$$\tau_N = R_{thN} C_{thN} \tag{1}$$

For the thermal structures it is the approximation due to the inherently distributed nature. In order to maintain usefulness in the model generation of the time constant representation, the notion of the time-constant spectrum is introduced [13]. This spectrum is a function which shows the intensity values of the time-constants of the distributed system. The spectra may be classified into two groups: discrete and continuous (fig. 4a and b, respectively).

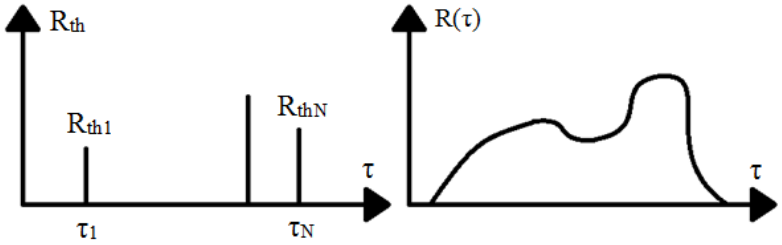

Fig. 4.*Time constants in a lumped element system (a) and in a distributed parameter system (b) [9]*

The simplest model consists of one RC cell. If one assumes the power step excitation *P,* the temperature will rise in conformity with (2), where the time constant τ is equal to $R_{th}C_{th}$.

$$T(t) = PR_{th}\left[1 - exp\left(-\frac{t}{\tau}\right)\right] \tag{2}$$

However, the real structure can consist of more than one time constant, then equation (2) will be expressed by equation (3). It suggests that, the infinitesimal part of the structure corresponds to the infinitesimal thermal resistance and capacity.

$$T(t) = P\sum_{i=1}^{N} R_{thi}\left[1 - exp\left(-\frac{t}{\tau_i}\right)\right] \tag{3}$$

10.21611/qirt.2016.062

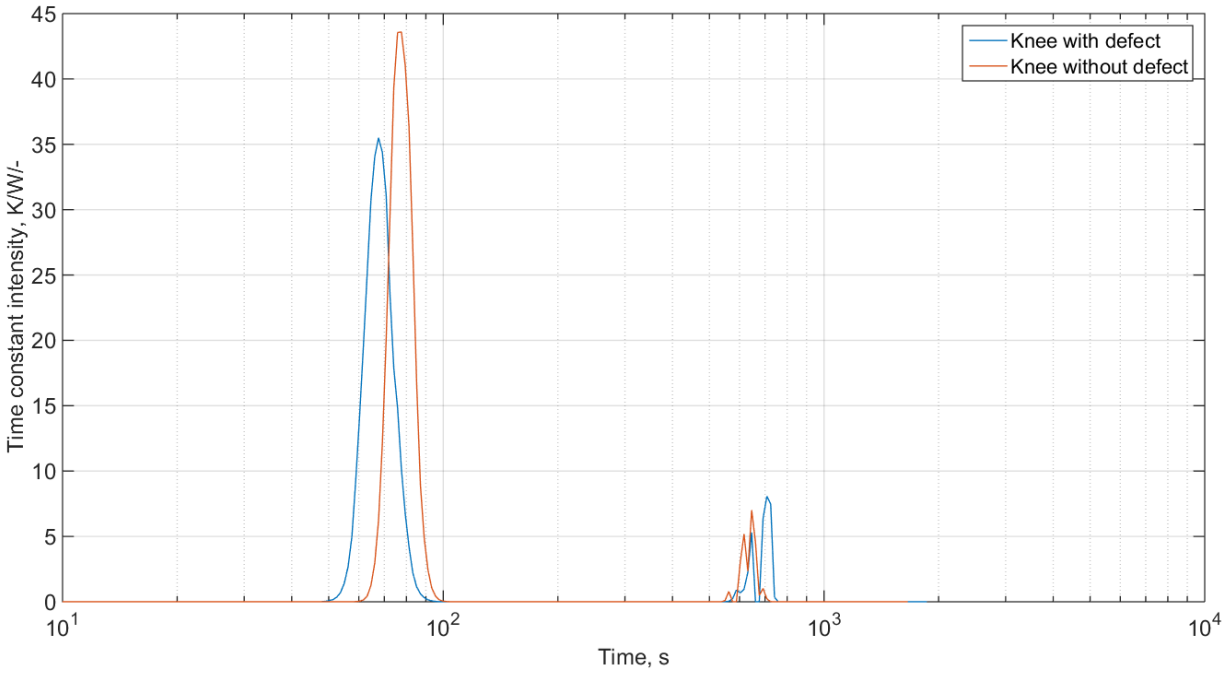

Fig. 5. *The thermal time constant intensity diagram*

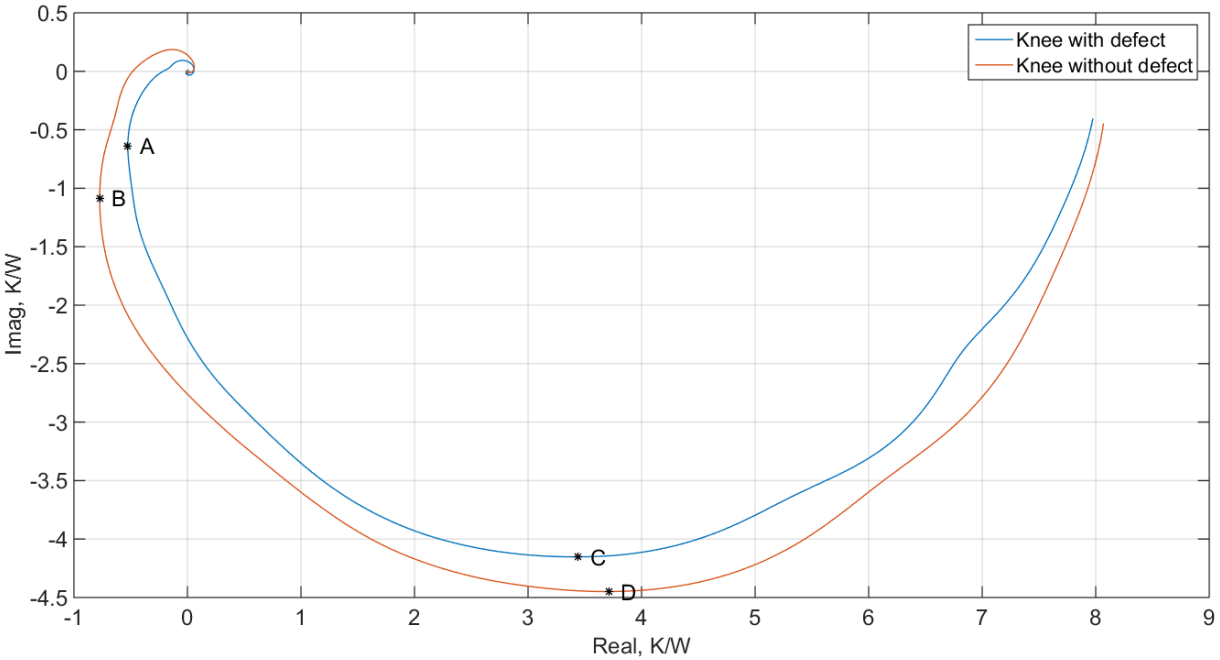

Fig. 6. *The Nyquist plots of the thermal impedance for the knees with different wall thickness*

The characteristics of the surface temperature changes are presented in tab. 1 and 2.

Table 1. *An example of temperature changes range for the whole heating process of the pipe wall*

	Knee with defect	Knee without defect	$\frac{Knee\ with\ defect}{Knee\ without\ defect} * 100,\ \%$
T_{max}, °C	42,19	37,61	112,18
T_{mean}, °C	39,80	36,53	108,95

Table 2. *An example of temperature changes range in the quasi-static condition of the pipe wall*

	Knee with defect	Knee without defect	$\frac{Knee\ with\ defect}{Knee\ without\ defect} * 100$, %
T_{min}, °C	38,80	36,53	106,21
T_{max}, °C	42,19	38,89	108,49
T_{mean}, °C	41,33	38,27	108,00
T_{std}, °C	0,64	0,39	164,10

Symbols in tables 1,2 denote: T_{min} - minimum, T_{max} - maximum, T_{mean} - mean , T_{std} - standard deviation of the temperature.

Table 3. *The values read from time constant intensity diagram and Nyquist plots*

	Knee with abraded wall (A, C points)	Knee without defect (B, D points)
τ, s	68,97	77,62
X_L, K/W	-0,53	-0,77
Y_L, K/W	-0,64	-1,09
ω_L, rad/s	0,13	0,78
φ_L, °	50,61	54,57
X_{BOTTOM}, K/W	3,44	3,71
Y_{BOTTOM}, K/W	-4,15	-4,45
ω_{BOTTOM}, rad/s	0,02	0,01
φ_{BOTTOM}, °	-50,36	-50,17
$1/\tau$, 1/s	0,02	0,01

The symbols in table 3 denote: τ - time constant; (X_{BOTTOM},Y_{BOTTOM}) - bottom point coordinates on the Nyquist plots, ω_{BOTTOM}, φ_{BOTTOM} - angular frequency and slope angle for the bottom points of Nyquist plot (C, D – fig. 6), (X_L,Y_L) - left points coordinates on the Nyquist plot (A, B – fig.6), ω_L, φ_L - angular frequency and slope angle for the left points of Nyquist plot

Finally the differential structure functions are presented (fig. 7). This diagram shows that the thermal resistance of the pipelines is variable, dependent on the wall thickness.

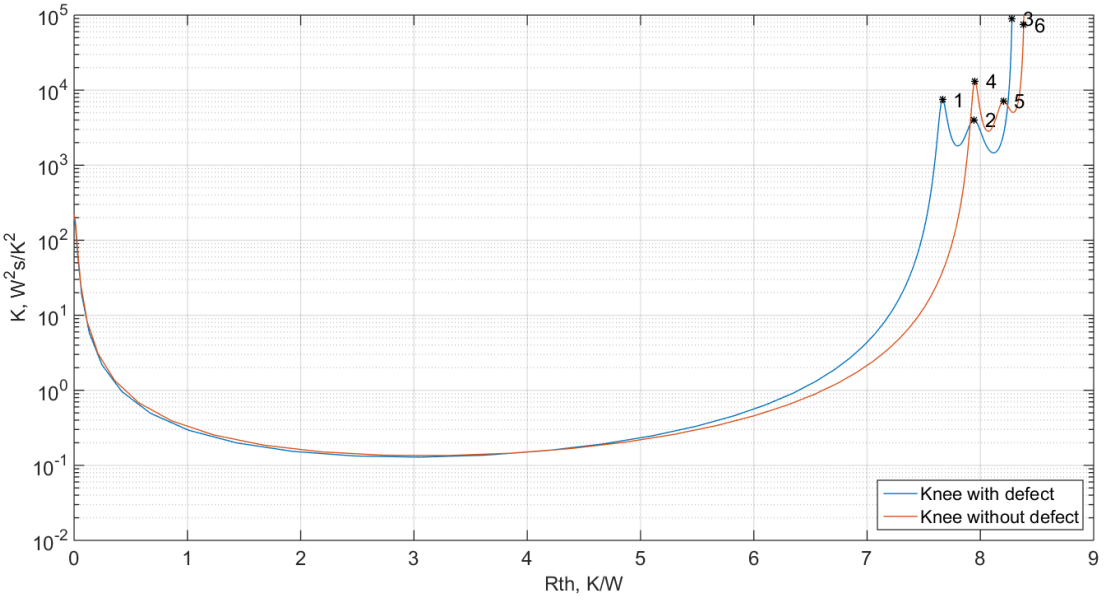

Fig. 7. *The differential structure functions*

3. Analysis

In this paper the pipes of different wall thickness without insulator were analyzed. In fig. 2 the heating process is shown. On this basis, one can notice that the mean value of the temperature in quasi-static condition for pipe with abraded wall has higher value. This phenomenon is associated with thermal resistance parameter R_{th}. Generally, the thermal resistance is a property of the material corresponding to the heat transfer. It is given by the ratio of the temperature difference ΔT between two points of the observed surface and the power P, which causes temperature difference (4).

$$R_{th} = \frac{\Delta T}{P} \tag{4}$$

The thermal resistance determinates the heat flow limit through the material of a certain thickness. On the basis (4) and fig. 7 one can conclude that the higher material thickness, the higher value of the thermal resistance is.

The next step of the analysis is describing the transient and frequency domain behavior. The measured data were imported to the T3Ster software. On the Nyquist characteristics (fig. 6), the curves are close to the semi-circle shapes. It confirms that the pipes could be characterized by a single RC stage. In the first iteration power step parameter was specified as the experimental value. Obviously, the thermal time constant value doesn't depend on power step parameter. The following analysis allows to determine the correct value of the power step and the knee wall thickness with defect. The analysis was performed up to the quasi-static condition.

It was assumed that the heat source has constant power (doesn't changes over time) and the barrier separates the regions of temperature T_x and T_m - fig. 8. We assumed that the heat transfer in one-dimensional direction only is, as shown in fig. 8. The temperature is a function of a coordinate measured along axis, which is perpendicular to the barrier and the density of the heat flux q is constant along the whole surface of the barrier. The phenomenon of the heat transfer occurs from the medium center (X), through the barrier, to the ambient center (A), where:

- T_a - ambient temperature,
- T_m - measured temperature,
- T_o - temperature of the air streams,
- T_x - temperature of the barrier from the side of the air streams.

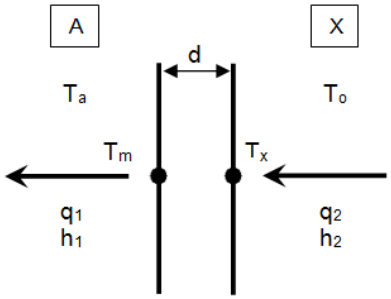

Fig. 8. *The cross-sectional view of the barrier with designations illustrating heat transfer*

The heat flow is a form of the energy exchange and occurs from area of higher temperature (T_x) to area of lower temperature (T_m). It is known that the amount of the energy (heat flux) q, which is transmitted through the barrier is dependent on thermal conductivity λ, temperature difference and the thickness of the barrier d and is expressed by Fourier law (5). During the experimental procedure, the temperature changes were relatively small, therefore it was assumed that the thermal conductivity is constant and independent of the temperature, equal 0,16 W/mK.

$$q = \lambda \frac{\Delta T}{d} \tag{5}$$

Knowing that the heating power P is expressed by (6) and the heat flux q by (5) is possible to calculate the heating power P, where S is surface of the heat transfer region.

$$P = q * S \tag{6}$$

Consequently, the equation (7) is obtained, (unit is Watt).

$$P = \lambda \frac{T_x - T_m}{d} * S \tag{7}$$

where, temperature T_x is determined from (11). The heat flux q is equal to the product of the heat transfer coefficient and temperature difference on the border between two centers. The heat flux in the medium center is expressed (8) and in the ambient center (9), respectively.

$$q_1 = h_2(T_o - T_x) \tag{8}$$

$$q_2 = h_1(T_m - T_a) \tag{9}$$

The same amount of the heat is transferred from the medium center to the ambient center, therefore the heat flux (8) is the same as the heat flux (8). Then it is obtained (10).

$$h_1(T_m - T_a) = h_2(T_o - T_x) \tag{10}$$

After simple transformation the T_x value was determined (11). The unit is Celsius degree.

$$T_X = T_o - \frac{h_1(T_m - T_a)}{h_2} \tag{11}$$

Finally step of the analysis is calculating of the abraded wall thickness. On the basis of data from table 3, we know that the time constant τ_1 for abraded wall is equal 68,97 s. and the time constant τ_2 for non-abraded wall is equal 77,60 s. The time constant is the result of the thermal resistance R_{th} and the heat capacity C_{th} multiplication, given by (12).

$$\tau = R_{th} * C_{th} \tag{12}$$

Subsisting power P from the (7) into (4) may be calculate the thermal constant value (13), taking wall thickness d, thermal conductivity λ, surface of the heat transfer S into consideration. While the heat capacity is the result of the volume V, density ϱ and the specific heat c_p multiplication (14).

$$R_{th} = \frac{\mathrm{d}}{\lambda S} \tag{13}$$

$$C_{th} = V * \varrho * c_p \tag{14}$$

where the volume is equal (15).

$$V = S * d \tag{15}$$

Considering (13), (14) and (15) the time constant equation is obtained (16).

$$\tau = \frac{d^2 * \varrho * c_p}{\lambda} \tag{16}$$

Measuring the time constants value τ_1 and τ_2 for walls with and without defects and wall thickness d_1 for the wall without defect, one may be determined wall thickness d_2 with abrasion (17) and (18).

$$\frac{\tau_1}{\tau_2} = \frac{d_1^2}{d_2^2} \tag{17}$$

$$d_2 = \sqrt{\frac{\tau_2 * d_1^2}{\tau_1}} \tag{18}$$

Based on the presented analysis, the temperature T_x, power P, thermal resistance R_{th}, heat capacity C_{th} and time constant τ parameters for both cases can be calculated. It is assumed that h_1 = 20 $\frac{W}{m^2K}$, h_2 = 100 $\frac{W}{m^2K}$, T_o = 73°C, T_m = 37,78°C for knee with defect, T_m = 38,52°C for knee without defect, λ = 0,16 $\frac{W}{mK}$, S = 25 cm^2, d_1 = 2,25 mm, c_p = 900 $\frac{J}{kgK}$, ϱ = 2000 $\frac{kg}{m^3}$ and T_a = 0°C. The obtained results are shown in tab. 4. Finally, the wall thickness with defect is estimated d_2 = 2,12 mm.

Table 4. *The obtained results of the analysis*

	Knee with defect	Knee without defect
T_x, °C	65,44	65,30
P, W	5,22	4,76
R_{th}, °C/W	5,30	5,63
C_{th}, J/K	9,54	10,13
τ, s	56,95	50,56

The differential structure function (DSF) have been also analyzed (fig. 7). The whole thermal path is divided by several sections. The total thermal resistance is a sum of the resistances for the particular studied layers. The left-hand of the curves (fig. 7) refers to the medium, the right-hand to the ambient. It was applied the division of the differential structure function. One can divide DSF into 3 regions: from the air streams to the internal PP surface (from the left-hand part to point 1), PP wall (from point 1 to point 2) and outer PP surface to the air (from point 2 to point 3) for knee without

defect. After locating these characteristic points, the partial resistances values can be read from the fig. 7. The thermal resistances of the system were shown in tab. 5.

Table 5 *The thermal resistance values R_{th} and value of the differential structure function K read from the DSF*

Knee with abraded wall			Knee without defect		
Point no.	R_{th}, °C/W	K, W^2s/K^2	Point no.	R_{th}, °C/W	K, W^2s/K^2
1	7,67	7482,29	4	7,95	13165,00
2	7,94	4024,00	5	7,94	7171,03
3	8,28	89803,00	6	8,28	74376,10

Knee with abraded wall		Knee without defect	
R_{th1-2}, °C/W	0,28	R_{th4-5}, °C/W	0,25
R_{th2-3}, °C/W	0,33	R_{th5-6}, °C/W	0,18

4. Conclusions

In this article two PP knees of different wall thickness were studied. The presented results and the analysis of the thermographic measurements indicate the possibility of estimating wall thickness in the pipelines. The studies were performed for bended segments of the pipeline. The following conclusions can be drown form this preliminary research.

- The thermal impedance analysis is the useful tools for this type of the study using transient thermography.
- The dynamic behavior was proved by the thermal transient tests. The single dominant time constants was found (fig. 5).
- On the basis of the Nyquist characteristics, the angular frequency ω_B should be approximately equal to $1/\tau$ [14,15]. The data from table 3 confirms this relationship. Comparing the data for two wall thickness, one can confirm that the phase delay φ_B is lower for smaller wall thickness.
- The differential structure functions was analyzed. It shows that differences of the thermal characteristics occur.

This presented research results shows how material parameter can be determined by transient testing. The analysis should be treated with the limited confidence due to random factors influence on the measurement. The uncertainty analysis has to be included in the next step of the research.

REFERENCES

[1] Pluvinage G., "General approaches of pipeline defect assessment", Chapter, Safety, Reliability and Risks Associated with Water, Oil and Gas Pipelines, Part of the series NATO Science for Peace and Security Series, pp 1-22.

[2] Weil G. J., Graf R J., "Infrared-thermography-based pipeline leak detection system", Proc. SPIE 1467, Thermosense XIII, (1 March 1991).

[3] Frank M., Hans R., Helmut S., "Experience with piping in German NPPs with respect to ageing-related aspect", Nucl. Eng. & Des., vol. 207, pp. 307-316 (2001).

[4] Kim K. S., Chang H. S., Hong D. P., Park C. J., Na S. W., Kim K. S., Jung H. C., "Defect detection of the wall thinning pipe of the nuclear power plant using infrared thermography", of the Korean Society for Nondestructive Testing, vol. 30, pp. 85-90 (2010).

[5] Shen G., Li T., "Infrared thermography for high-temperature pressure pipe", Insight, vol. 49, pp. 151-153, (2007).

[6] Łabanowski J., "Ocena procesów niszczenia rur katalitycznych w eksploatacji reformerów metanu", Wydawnictwo Politechniki Gdańskiej, ISBN 83-7348-039-0, Wydanie I, Ark. wyd. 6, 4. Arkusz druku 6, 5, Gdańsk (2003).

[7] Altair User Manual, Cedip Infrared Systems, Version 5.90.002, (8 January 2010).

[8] T3Ster® Measurement Control Tool User and Reference Guide, Software Version 1.3, (January 17, 2014).

[9] Székely V., Rencz M. "Thermal dynamics and the time constant domain", IEEE Transactions on Components and Packaging Technologies, vol. 23, pp. 587-594, (no. 3. September 2000).

[10] Matlab User Manual, Version 8.0, (September 2012).

[11] Bognár Gy., Fürjes P., Székely V., Rencz M., "Transient thermal characterization of the hot plates", Microsyst Technol, (February 2005), pp. 154-159.

[12] Rencz M., "New possibilities in the thermal evaluation, offered by transient testing", Microelectronics Journal 34, (2003), pp. 171-177.

[13] Kopeć M., "The application of the infrared camera to verification of the documents authenticity", VI Wyjazdowa Sesja Naukowa Doktorantów Politechniki Łódzkiej, Rogów 2016, pp. 81-87, (April 2016).

[14] Vermeersch B., De Mey G., "Influence of substrate thickness on thermal impedance of microelectronics structures", Microelectronics reliability, no. 47/2007, pp. 437-443.

[15] Chatziathanasiou V., Chatzipanagiotou P., Papagiannopoulos I., De Mey G., Więcek B., "Dynamic thermal analysis of underground medium power cables using thermal impedance, time constant distribution and structure function", Applied Thermal Engineering, no. 60/2013, pp. 256 - 260.